

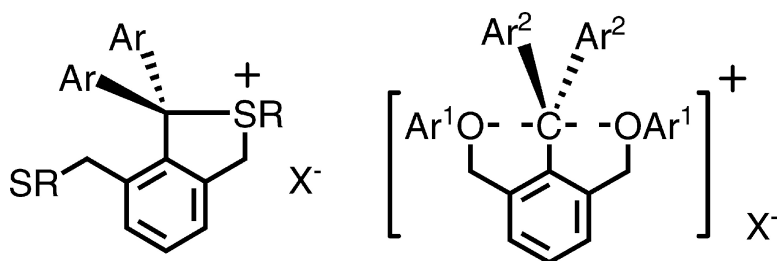
Article

Synthesis and Characterization of Stable Hypervalent Carbon Compounds (10-C-5) Bearing a 2,6-Bis(*p*-substituted phenyloxymethyl)benzene Ligand

Kin-ya Akiba, Yuji Moriyama, Mitsuhiro Mizozoe, Hideki Inohara, Takako Nishii, Yohsuke Yamamoto, Mao Minoura, Daisuke Hashizume, Fujiko Iwasaki, Nozomi Takagi, Kazuya Ishimura, and Shigeru Nagase

J. Am. Chem. Soc., **2005**, 127 (16), 5893-5901 • DOI: 10.1021/ja043802t • Publication Date (Web): 02 April 2005

Downloaded from <http://pubs.acs.org> on March 25, 2009



More About This Article

Additional resources and features associated with this article are available within the HTML version:

- Supporting Information
- Links to the 8 articles that cite this article, as of the time of this article download
- Access to high resolution figures
- Links to articles and content related to this article
- Copyright permission to reproduce figures and/or text from this article

[View the Full Text HTML](#)

Synthesis and Characterization of Stable Hypervalent Carbon Compounds (10-C-5) Bearing a 2,6-Bis(*p*-substituted phenyloxymethyl)benzene Ligand

Kin-ya Akiba,^{*,‡} Yuji Moriyama,[†] Mitsuhiro Mizozoe,[†] Hideki Inohara,[†] Takako Nishii,[†] Yohsuke Yamamoto,^{*,†} Mao Minoura,[†] Daisuke Hashizume,[§] Fujiko Iwasaki,[§] Nozomi Takagi,^{||} Kazuya Ishimura,^{||} and Shigeru Nagase^{||}

Contribution from the Department of Chemistry, Graduate School of Science, Hiroshima University, 1-3-1 Kagamiyama, Higashi-Hiroshima 739-8526, Japan, Advanced Research Center for Science and Engineering, Waseda University, 3-4-1 Ohkubo, Shinjuku-ku, Tokyo 165-8555, Japan, Department of Applied Physics and Chemistry, The University of Electro-Communications, 1-5-1 Chofugaoka, Chofu, Tokyo 182-8585, Japan, and Department of Theoretical Molecular Science, Institute for Molecular Science, Myodaiji, Okazaki 444-8585, Japan

Received November 30, 2004; E-mail: yyama@sci.hiroshima-u.ac.jp

Abstract: X-ray analysis of bis(*p*-fluorophenyl)methyl cation bearing a 2,6-bis(*p*-tolylloxymethyl)benzene ligand showed a symmetrical structure (10-C-5) where the two C–O distances are identical, although the distance (2.690(4) Å) is longer than those (2.43(1) and 2.45(1) Å) of 1,8-dimethoxy-9-dimethoxymethyl-anthracene monocation, which was recently reported by us. However, X-ray analysis of the more stable aromatic xanthylium cation with the same benzene ligand showed the tetracoordinate carbon structure where only one of the two oxygen ligands is coordinated with the central carbon atom. These results clearly indicate that the carbocations (10-C-5) bearing the sterically flexible benzene ligand were quite sensitive to the electronic effect on the central carbon atom. The electron distribution analysis by accurate X-ray measurements and the density functional calculation on the initially mentioned bis(*p*-fluorophenyl)methyl cation clearly show that the central carbon atom and the two oxygen atoms are bonded even if the bond is weak and ionic based on the small value of the electron density ($\rho(r)$) and the small positive Laplacian value ($\nabla^2\rho(r)$) at the bond critical points.

Introduction

The chemistry of hypervalent compounds has been acquiring wider and deeper attention both by organic chemists and by inorganic chemists as a new and rapidly developing area between the two fields during the past 20 years.¹ Especially, during active experimental investigations on the organic chemistry of silicon,² phosphorus,³ sulfur,⁴ and iodine,⁵ several new, unique but fundamental features of structures and reaction patterns have been found to commonly occur to the organic

compounds of these elements. In 1951, theoretical interpretation of the structure of $[I-I-I]^-K^+$ and its analogues was proposed on the basis of the three-center four-electron (3c-4e) bond using molecular orbital theory.^{6a} The three-center four-electron (3c-4e) bond has been called a hypervalent bond and consists of an apical bond of a pentacoordinate trigonal bipyramidal molecule where a hypervalent bond is most typically seen.^{6b} To experimentally create a 3c-4e bond of pentacoordinate molecules, three methods can be considered (Scheme 1): (i) add two free radicals to coordinate with a pair of unshared electrons in a p orbital; (ii) add two pairs of unshared electrons (nucleophiles) to

[†] Hiroshima University.

[‡] Waseda University.

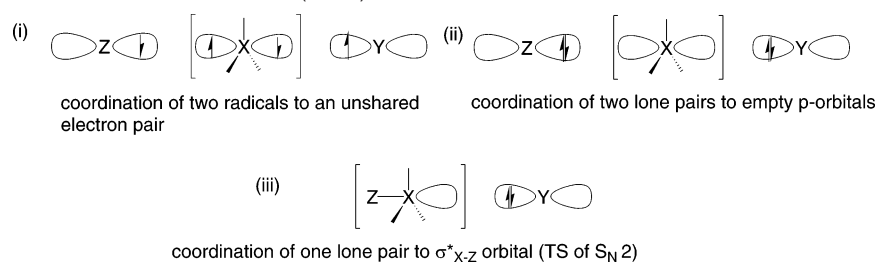
[§] The University of Electro-Communications.

^{||} Institute for Molecular Science.

- (1) (a) Akiba, K.-y. *Chemistry of Hypervalent Compounds*; Wiley-VCH: New York, 1999. (b) Block, E. *Heteroatom Chemistry*; VCH: New York, 1990.
- (2) (a) Corriu, J. P. In *Chemistry of Hypervalent Compounds*; Akiba, K.-y., Ed.; Wiley-VCH: New York, 1999; Chapter 4, pp 81–146 and references therein. (b) Kira, M.; Zhang, L. C. In *Chemistry of Hypervalent Compounds*; Akiba, K.-y., Ed.; Wiley-VCH: New York, 1999; Chapter 5, pp 147–169 and references therein.
- (3) (a) Holmes, R. R. *Pentacoordinated Phosphorus—Structure and Spectroscopy*; ACS Monograph 175, 176; American Chemical Society: Washington, DC, 1980; Vols. 1, 2. (b) Corbridge, D. E. C. *Phosphorus: An Outline of Its Chemistry, Biochemistry, and Technology*, 4th ed.; Elsevier: Amsterdam, 1990; Chapter 14, pp 1233–1256. (c) Burgada, R.; Setton, R. In *The Chemistry of Organophosphorus Compounds*; Hartley, F. R., Ed.; Wiley-Interscience: Chichester, 1994; Vol. 3, pp 185–272. (d) Kawashima, T. In *Chemistry of Hypervalent Compounds*; Akiba, K.-y., Ed.; Wiley-VCH: New York, 1999; Chapter 6, pp 171–210 and references therein.

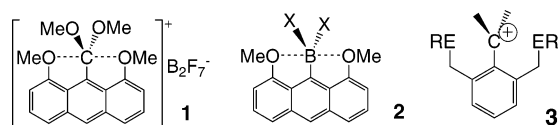
- (4) (a) Martin, J. C. *Science* **1983**, 221, 509–514. (b) Drabowicz, J. In *Chemistry of Hypervalent Compounds*; Akiba, K.-y., Ed.; Wiley-VCH: New York, 1999; Chapter 7, pp 211–240 and references therein. (c) Furukawa, N.; Sato, S. In *Chemistry of Hypervalent Compounds*; Akiba, K.-y., Ed.; Wiley-VCH: New York, 1999; Chapter 8, pp 241–278 and references therein. (d) Lentz, D.; Seppelt, K. In *Chemistry of Hypervalent Compounds*; Akiba, K.-y., Ed.; Wiley-VCH: New York, 1999; Chapter 10, pp 295–326 and references therein.
- (5) (a) Zhdankin, V. V.; Stang, P. In *Chemistry of Hypervalent Compounds*; Akiba, K.-y., Ed.; Wiley-VCH: New York, 1999; Chapter 11, pp 327–358 and references therein. (b) Ochiai, M. In *Chemistry of Hypervalent Compounds*; Akiba, K.-y., Ed.; Wiley-VCH: New York, 1999; Chapter 12, pp 359–388 and references therein. (c) Varvoglis, A. *The Chemistry of Polycordinated Iodine*; VCH: New York, 1992.
- (6) (a) Pimentel, G. C. *J. Chem. Phys.* **1951**, 19, 446. Hackand, R. J.; Rundle, R. E. *J. Am. Chem. Soc.* **1951**, 73, 4321. (b) Musher, J. I. *Angew. Chem., Int. Ed. Engl.* **1969**, 8, 54–68.

Scheme 1. Creation of a Three-Center Four-Electron (3c-4e) Bond of Pentacoordinate Molecules



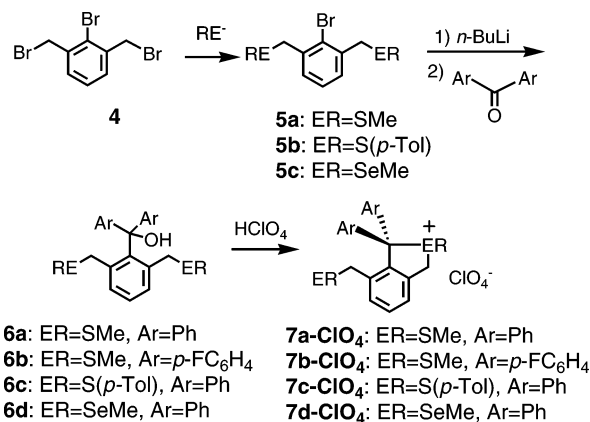
coordinate with a vacant p orbital; or (iii) add a pair of unshared electrons to coordinate with the σ^* orbital of an X–Z bond in a cationic or neutral molecule. When X is a carbon, method (iii) corresponds to the formation of the transition state (TS) of the S_N2 reaction.

Recently, we reported the first fully characterized pentacoordinate hypervalent 10-C-5⁷ carbon compound (**1**)⁸ and the 10-B-5 boron compounds (**2**)⁹ bearing a sterically rigid 1,8-dimethoxyanthracene ligand, which correspond to method (ii) above. The X-ray results [the two O–C distances are almost identical (2.43(1) and 2.45(1) Å) in **1**, and the O–B distances are 2.405(6) and 2.462(6) Å in **2** (X = OMe)] and the hybrid density functional theory (DFT) calculation of **1** and **2** clearly showed the presence of an attractive interaction between the central carbon (or the boron) atom and the oxygen atoms at the 1,8 positions, although the C(or B)–O bond is weak and ionic.^{8,9} The bonding nature of the central carbon (or the boron) atom and the coordinating oxygen atoms bearing an anthracene ligand will be discussed in a separate paper.^{9c}

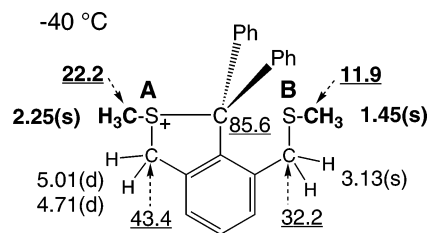


Instead of the sterically rigid anthracene derivatives, here we report the synthesis and crystal structures of carbocations (**3**) having a series of newly prepared 2,6-bis(substituted)methylbenzene ligands.¹⁰ Among the series, compounds **7a–7d** (Scheme 2) bearing two SMe, S(*p*-Tol) (*p*-Tol: *p*-CH₃C₆H₄), and SeMe groups showed unsymmetrical structures where only one of the two sulfurs (or seleniums) coordinated with the central carbon atom resulting in sulfonium (or selenonium) salts. However, X-ray analysis of sterically flexible **15b-ClO₄**, **15c-ClO₄**, and **15e-ClO₄** bearing two O(*p*-Tol) groups and **16a-ClO₄**, **16b-PF₆**, and **16d-PF₆** bearing two O(*p*-CH₃OC₆H₄) groups (Scheme 5 and Table 2) showed symmetrical structures where the two O–C distances are almost identical, although the two O–C distances (2.6–2.9 Å) are even longer than those of **1**. The attractive O–C interaction between the central carbon

Scheme 2. Synthesis of Carbocations Bearing 2,6-Bis(sulfur- or selenium-substituted)methylbenzene



and the two O(*p*-Tol) groups in **15b-ClO₄** was clarified by electron-distribution analysis based on accurate X-ray measurements and DFT calculation.



¹H and ¹³C NMR Spectra Data (CD₃CN, ppm)

Figure 1. ¹H and ¹³C NMR spectra of **7a-ClO₄** at $-40\text{ }^\circ\text{C}$ (CD₃CN).

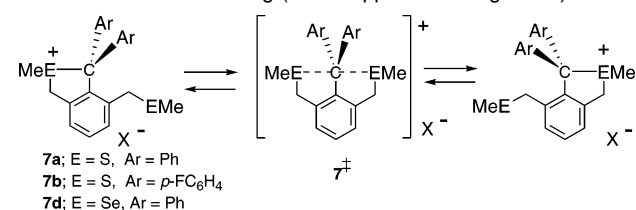
Scheme 3. Bond Switching (Bell Clapper Rearrangement) in **7**

Table 1. Activation Parameters for the Bond Switching Process in **7**

	solvent	ΔG^\ddagger_{298} (kcal/mol)	ΔH^\ddagger (kcal/mol)	ΔS^\ddagger (eu)	T_c (K)
7a (TFPB)	CD ₂ Cl ₂	11.4	13.1 ± 0.1	5.6 ± 0.2	259
7a (TFPB)	CD ₃ CN	13.9	15.3 ± 0.1	4.6 ± 0.2	303
7b (ClO ₄)	CD ₃ CN	13.7	13.3 ± 0.1	-1.2 ± 0.1	297
7b (ClO ₄) ^a	CD ₃ CN	13.8	12.8 ± 0.1	-3.5 ± 0.2	311
7b (TFPB)	CD ₂ Cl ₂	11.7	10.2 ± 0.2	-5.2 ± 0.6	249

^a Based on ¹⁹F NMR.

- (7) For N–X–L designation: X, central atom; N, formal valence-shell electrons about an X; L, the number of ligands. Perkins, C. W.; Martin, J. C.; Arduengo, A. J.; Lau, W.; Alegria, A.; Kochi, J. K. *J. Am. Chem. Soc.* **1980**, *102*, 7753.
- (8) (a) Akiba, K.-y.; Yamashita, M.; Yamamoto, Y.; Nagase, S. *J. Am. Chem. Soc.* **1999**, *121*, 10644. (b) Yamashita, M.; Kamura, K.; Yamamoto, Y.; Akiba, K.-y. *Chem.-Eur. J.* **2003**, *9*, 3655–3659.
- (9) (a) Yamashita, M.; Yamamoto, Y.; Akiba, K.-y.; Nagase, S. *Angew. Chem., Int. Ed.* **2000**, *39*, 4055–4058. (b) Yamashita, M.; Watanabe, K.; Yamamoto, Y.; Akiba, K.-y. *Chem. Lett.* **2001**, 1104–1105. (c) Yamashita, M.; Yamamoto, Y.; Akiba, K.-y.; Hashizume, D.; Iwasaki, F.; Takagi, N.; Nagase, S. *J. Am. Chem. Soc.* **2005**, *127*, in press.
- (10) (a) Albrecht, M.; van Koten, G. *Angew. Chem., Int. Ed.* **2001**, *40*, 3750–3781. (b) Albrecht, M.; Kochs, B. M.; Spek, A. L.; van Koten, G. *J. Organomet. Chem.* **2001**, *624*, 271–286.

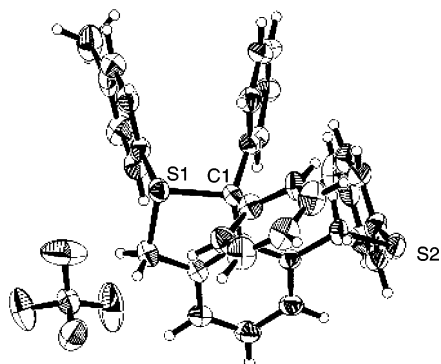


Figure 2. ORTEP drawing of 7c-ClO₄.

Results and Discussion

Preparation of Sulfur and Selenium Ligands and of the Corresponding Carbocation Derivatives: Observation of Bond Switching Process. Sulfur and selenium ligands (**5a–5c**) were prepared from the tribromide (**4**) in good yields (Scheme 2). The corresponding lithium salt from **5** reacted with benzophenone derivatives to give the corresponding alcohols (**6a–6d**) (yield: 51–87% for **6a–6c** and 14% for **6d**, respectively). Treatment of **6a–6d** with perchloric acid gave the corresponding cations, **7a–7d**, as a perchlorate almost quantitatively.

In solutions of **7a–7d**, two sets of signals for the sulfur substituents, the methylene groups, and the meta carbons (or protons) on the trisubstituted phenyl ring were observed at low temperatures, although only one set of symmetrical signals was observed at higher temperatures. For example, two sharp singlets for the S–CH₃ protons (δ 1.45, 2.25) and carbons (δ 11.9, 22.2) in ¹H and ¹³C NMR spectra were observed in **7a-ClO₄** at –40 °C (CD₃CN) (Figure 1), but coalescence took place at 30 °C in ¹H NMR. At higher temperatures (100 °C), two sharp singlets of the S–CH₃ (δ 2.05) and S–CH₂ protons (δ 4.02) were observed for the same sample.

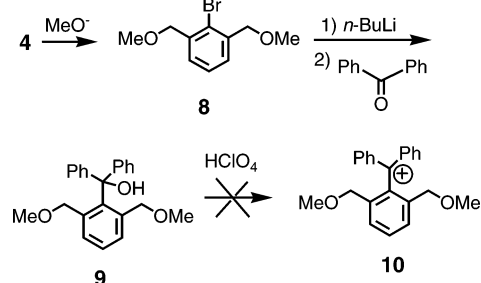
These results indicated that the ground state of the compounds should be a tetracoordinated structure at the central carbon atom, and the bond switching (bell clapper rearrangement) took place as illustrated in Scheme 3. The activation free energies (ΔG^\ddagger) of the process for **7a-TFPB** and **7d-TFPB** [TFPB: tetrakis-{3,5-bis(trifluoromethyl)phenyl}borate] were determined on the basis of the simulation of the coalescence of the methyl signals. The activation free energies (ΔG^\ddagger) are shown in Table 1 together with the coalescence temperature (T_c). The activation free energies were almost the same in CD₂Cl₂ in the sulfur and selenium ligand; thus, ΔG_{298}^\ddagger was 11.4 kcal/mol (T_c (coalescence temperature) = 259 K in 400 MHz ¹H NMR) for **7a-TFPB**, and $\Delta G_{298}^\ddagger = 11.7$ kcal/mol ($T_c = 249$ K) for **7d-TFPB**. It should be noted that **7a-ClO₄** showed the same coalescence temperature as **7a-TFPB**. Therefore, the counteranion should not be interacted with the cationic part. In polar CD₃CN solution, activation energies were higher by ca. 2.5 kcal/mol because of the stabilization of the starting polarized onium structures. Therefore, the pentacoordinated carbon structure (**7⁺**) should be the transition state of the bond switching process.

Consistent with the NMR behavior in solution, the X-ray crystal structures of **7a-ClO₄** or **7c-ClO₄** clearly show that only one of the sulfur atoms is coordinated with the central carbon

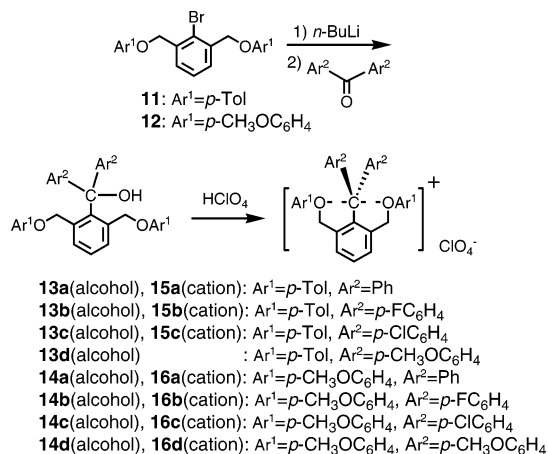
atom to give a sulfonium salt. The X-ray structure of **7c-ClO₄** is shown in Figure 2 (bond distance: S¹–C¹ = 1.973(8) Å, S²–C¹ = 4.86(1) Å), and the structure of **7a-ClO₄** (not shown) was similar to that of **7c-ClO₄**.

Preparation of Oxygen Ligands and of the Corresponding Carbocation Derivatives: Behaviors in Solution. The corresponding OMe ligand (**8**) and the alcohol (**9**) were prepared by similar procedures (Scheme 4), but demethylation and decomposition took place after the treatment of **9** with perchloric acid to give an unidentified mixture. Therefore, we prepared the corresponding O(*p*-Tol) alcohols, **13a–13d**, and O(*p*-MeOC₆H₄) alcohols, **14a–14d**. The corresponding cations, **15a–15c**, **16a–16d**, could be prepared almost quantitatively by treatment with perchloric acid (Scheme 5) (**15d** was very unstable and could not be isolated). The cations were somewhat unstable at room temperature (vide infra) in solution, but the dark green color persisted up to 0 °C for several hours.

Scheme 4. Attempted Synthesis of a Cation (**10**) Bearing 2,6-Bismethoxymethylbenzene

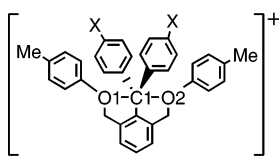
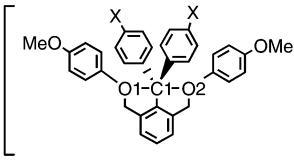
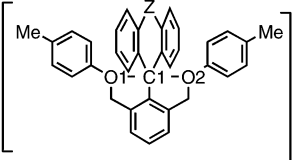


Scheme 5. Synthesis of Cations (**15a–c** and **16a–d**) Bearing 2,6-Bis(*p*-substituted phenyloxymethyl)benzene



In solutions of **15a–15c**, two sets of signals were observed only for the methylene group and the ortho and meta carbons of the central carbon substituents (Ar²) at low temperatures, although only one set of symmetrical signals including the meta carbons (or protons) on the trisubstituted phenyl ring was observed for other signals. Figure 3 shows the coalescence of the two sets of signals for the ortho and meta carbons of the central carbon substituents (Ar²: δ 130.2 and 131.4, 139.7, and 140.2) coalesced at –30 °C. These results are consistent with the propeller inversion (Scheme 6) at the aryl substituents (Ar²) in trityl cations as a similar inversion process was reported by

Table 2. Distances of the Central Carbon Atom (C¹) and the Donating Oxygen Atoms (O¹ and O²) and the O¹–C¹–O² Angles Revealed by X-ray Analysis of **15b**–ClO₄, **15c**–ClO₄, **15e**–ClO₄, **15f**–ClO₄, **16a**–ClO₄, **16b**–PF₆, and **16d**–PF₆

	 15b (X=F) ClO ₄ ⁻ 15c (X=Cl) ClO ₄ ⁻		 16a (X=H) 16b (X=F) 16d (X=OMe)		 15e (Z=S) ClO ₄ ⁻ 15f (Z=O) ClO ₄ ⁻		
distance (Å)	15c –ClO ₄ (X = Cl)	15b –ClO ₄ (X = F)	16a –ClO ₄ (X = H)	16b –PF ₆ (X = F)	16b –PF ₆ (X = OCH ₃)	15e –ClO ₄ (Z = S)	15f –ClO ₄ (Z = O)
C ¹ –O ¹	2.671(4)	2.690(4)	2.705(2)	2.718(5)	2.77(1)	2.776(4)	3.026(4)
C ¹ –O ²	2.682(4)	2.690(4)	2.705(2)	2.718(5)	2.78(1)	2.617(4)	4.23
O ¹ –C ¹ –O ²	161.9(1)	162.3(1)	158.9(2)	160.4(4)	159.1(4)	2.855(5)	2.827(4)
						155.7(2)	165.0(2)

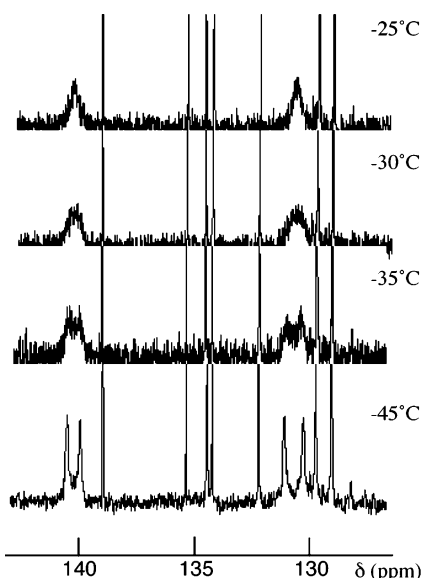


Figure 3. Variable-temperature ¹³C NMR (CD₂Cl₂) spectra of **15b**–ClO₄. Coalescence of the ortho and meta carbons of *p*-fluorophenyl substituents.

Breslow et al.^{11b} The barrier for inversion was $\Delta G_{Tc}^{\ddagger} = 11.7$ kcal/mol ($T_c = 249$ K) in CD₂Cl₂.

It is interesting to note that the cations **15a**–**15c** and **16a**–**16d** are colored solids, and the UV–vis spectra of **16a**–**16d** (mostly purple solid) showed interesting behavior (Figure 4). The wavelength of the absorption is shifted according to electron-withdrawing substituents (X) attached to the aryl substituents (*p*-XC₆H₄; Ar² in Scheme 5). Based on the calculated HOMO and LUMO orbitals in **15b**–ClO₄ (Figure 5), the substituent effect of the Ar² in **16** on the wavelength can be explained by HOMO (hybrid of the π -electrons of the aryl substituents (Ar¹) and the lone pair electrons of the oxygen atom of the ligand)–LUMO (hybrid of the empty p orbital of the central carbon atom and the aryl group (Ar²)) interaction. The energy of the LUMO orbital should be lowered by introducing the electron-withdrawing substituents on Ar² such as chlorine

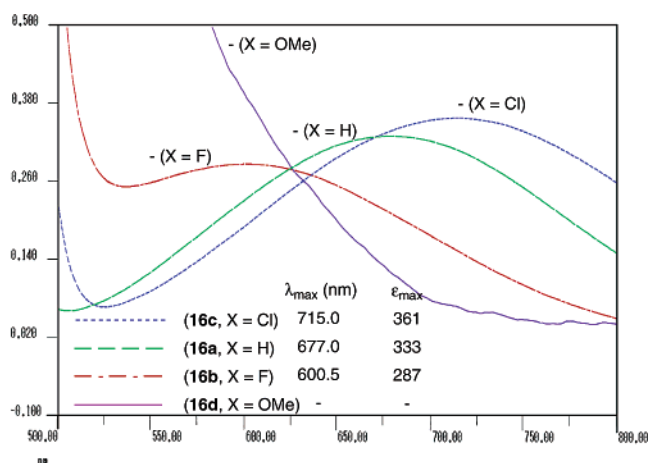
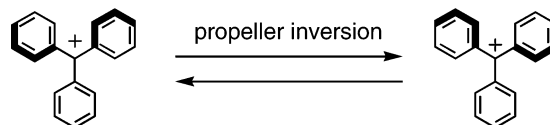


Figure 4. UV–vis spectra of **16a**–**16d**.

Scheme 6. Propeller Inversion at the Aryl Substituents (Ar²) in Trityl Cations



(X: σ^+ , Cl +0.07 (**16c**), H 0 (**16a**), F –0.11 (**16b**), CH₃O –0.78 (**16d**)), resulting in the smaller HOMO–LUMO energy gap and the absorption shifted to the longer wavelength.

X-ray Crystallographic Analyses of Several Carbocations Bearing O(*p*-Tol) or O(*p*-CH₃OC₆H₄) Ligand: Electronic Effects of the Aryl Substituents on the Central Carbon Atom Affected the C–O Distance and the Structure. The crystals of bis(*p*-fluorophenyl)[2,6-bis(*p*-methylphenyloxymethyl)phenyl]methyl perchlorate **15b**–ClO₄ suitable for X-ray analysis were obtained after careful recrystallization from CH₂Cl₂ in a freezer. X-ray structural analysis of **15b**–ClO₄ was carried out on the basis of the centrosymmetric *Pbcn* group, showing that the required two-fold axis passed through the central carbon and the two carbon atoms at ipso and para positions in the trisubstituted benzene ring. Figure 6 shows the ORTEP drawing

(11) (a) Breslow, R.; Garratt, S.; Kaplan, L.; LaFollette, D. *J. Am. Chem. Soc.* **1968**, *90*, 4051–4055. (b) Breslow, R.; Kaplan, L.; LaFollette, D. *J. Am. Chem. Soc.* **1968**, *90*, 4056–4064.

(12) (a) Becke, A. D. *Phys. Rev.* **1988**, *A38*, 3098–3100, (b) Becke, A. D. *J. Chem. Phys.* **1993**, *98*, 5648–5652, (c) Perdew, J. P.; Wang, Y. *Phys. Rev.* **1992**, *B45*, 13244–13249.

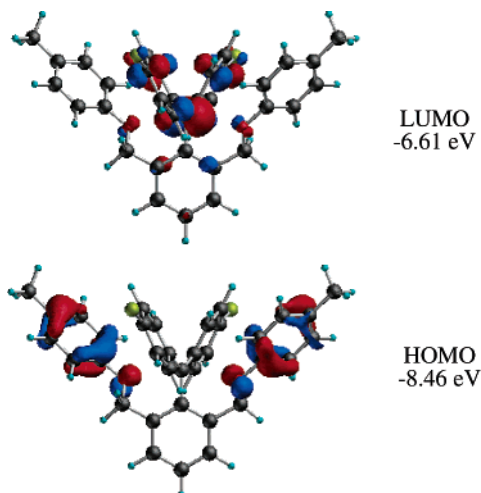


Figure 5. HOMO and LUMO orbitals of **15b** ($X = \text{F}$) calculated at the B3PW91/6-31G(d) level.

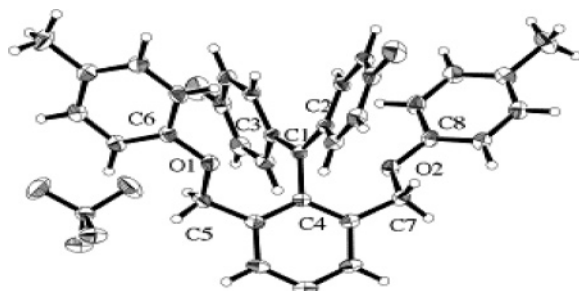
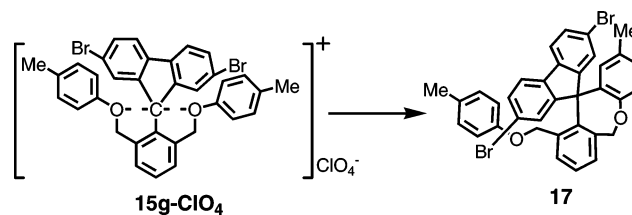


Figure 6. ORTEP drawing of **15b-ClO₄**.

of a single molecule of **15b-ClO₄**. Because of the symmetry, the bond distance between O1–C1 and O2–C1 is the same (2.690(4) Å), which is even longer than those of the C–O distances (2.43(1) and 2.45(1) Å) in **1** and is significantly longer than that of a covalent C–O bond (1.43 Å),¹³ but it is still shorter than the sum of the van der Waals radius (3.25 Å).¹³ The sum of the angles (C²–C¹–C⁴, C²–C¹–C³, and C³–C¹–C⁴) around the central carbon is 360.0°, indicating that the carbon is planar with sp² hybridization. Moreover, both oxygens (O¹ and O²) are sp²; that is, the sum of the angles (C⁵–O¹–C⁶, C¹–O¹–C⁶, C¹–O¹–C⁵) around O¹ is 360.0°. Because the sp² lone pairs of O¹ and O² should be directed toward the empty p-orbital of the central carbocation, the geometry around the central carbon atom C¹ is TBP, which is only slightly distorted. The 2p orbitals of O¹ and O² become parallel to the aromatic 6π system of the substituted benzene ligand and are perpendicular to the hypervalent bond of O¹–C¹–O².

To elucidate the property and the degree of interaction between the central carbon atom and the two oxygen atoms in **15**, several compounds were synthesized and were structurally characterized for comparison. Although the formation of the

Scheme 7. Intramolecular Friedel–Crafts Reaction in **15g-ClO₄**



fluorenyl cation derivative, **15g-ClO₄**, could be observed up to –20 °C, the dark green color disappeared at room temperature, and the intramolecular Friedel–Crafts product **17** was obtained (Scheme 7) almost quantitatively. The cyclopentadienyl cation system is more unstable than the trityl cation system. The structure of **17** was confirmed by X-ray analysis (not shown).

However, the more stable aromatic thioxanthylum cation **15e-ClO₄** and xanthylum cation **15f-ClO₄** could be isolated without any difficulty. X-ray analysis of **15e-ClO₄** (Figure 7) showed two independent molecules where the two C–O distances (first molecule, 2.617(4), 2.827(4) Å; second molecule, 2.776(4), 2.855(5) Å) are significantly different in the two molecules, indicating that the C–O interaction is very weak and the energy difference between the two molecules is small. Here, the thioxanthene ring is perfectly orthogonal to the substituted benzene ring of the ligand. In addition, it is quite interesting to note that the xanthene ring of **15f-ClO₄** is tilted to the uncoordinated arm and the central carbon looks like a tetracoordinate, although the C¹–O¹ length (3.026(4) Å) of the coordinated arm is quite long and is close to the sum of the van der Waals radii (3.25 Å) (Figure 8). Selected C–O distances and O–C–O angles are shown in Table 2. The aromatic xanthylum cation should be more stable than the thioxanthylum cation, and this is exemplified by the Hammett σ_p^+ values (–0.60 for SMe, and –0.78 for OMe). The difference of C–O attractive interaction between **15e-ClO₄** and **15f-ClO₄** is consistent with the less-attractive interaction between the central carbon and the oxygen atoms in **15f-ClO₄** (xanthylum) than in **15e-ClO₄** (thioxanthylum). The order of the C–O distance is **15c-ClO₄** ($X = \text{Cl}$) < **15b-ClO₄** ($X = \text{F}$) in the O(*p*-Tol) system and **16a-ClO₄** ($X = \text{H}$) < **16b-ClO₄** ($X = \text{F}$) < **16c-ClO₄** ($X = \text{CH}_3\text{O}$) in the O(*p*-CH₃OC₆H₄) system. It also agrees with the Hammett σ_p^+ values of the substituents (Cl +0.07, H 0, F –0.11, CH₃O –0.78). It is noteworthy that the C–O distance in **16b** (*p*-CH₃OC₆H₄ ligand) is almost the same as that in **15b** (*p*-tolyl ligand), because the two bond distances are within 3σ of each other.

Electron Density Distribution Study in 15b-ClO₄ Based on the Accurate X-ray Analysis. The accurate X-ray measurement of **15b-ClO₄** was carried out by using a Spring-8 beam line (see details in the Experimental Section). The structure and the C–O distance (2.6822(4) Å) are well consistent with the regular X-ray analysis described in Table 2 (2.690(4) Å). Figure 9 shows the static model map of **15b-ClO₄** on the plane intersecting the sp² plane of C1 perpendicularly along the C1–C4 bond.

The character of the O¹–C¹–O² bond (Figure 6) is clearly shown in the static model map. The topologies of deformation electron densities of the bond are quite different from those of the covalent bonds. As shown in Figure 9, the two lone pairs on each O atom in the O(*p*-tolyl) group appear as an electron-rich region (marked in blue) in the plane bisecting C⁶–O¹–C⁵

(13) Frisch, M. J.; Trucks, G. W.; Schlegel, H. B.; Scuseria, G. E.; Robb, M. A.; Cheeseman, J. R.; Zakrzewski, V. G.; Montgomery, J. A.; Stratmann, R. E., Jr.; Burant, J. C.; Dapprich, S.; Millam, J. M.; Daniel, A. D.; Kudin, S. K. N.; Strain, M. C.; Farkas, O.; Tomasi, J.; Barone, V.; Cossi, M.; Cammi, R.; Mennucci, B.; Pomelli, C.; Adamo, C.; Clifford, S.; Ochterski, J.; Petersson, G. A.; Ayala, P. Y.; Cui, Q.; Morokuma, K.; Malick, D. K.; Rabuck, A. D.; Raghavachari, K.; Foresman, J. B.; Cioslowski, J.; Ortiz, J. V.; Stefanov, B. B.; Liu, G.; Liashenko, A.; Piskorz, P.; Komaromi, I.; Gomperts, R.; Martin, L.; Fox, D. J.; Keith, T.; Al-Laham, M. A.; Peng, C. Y.; Nanayakkara, A.; Gonzalez, C.; Challacombe, M.; Gill, P. M. W.; Johnson, B.; Chen, W.; Wong, M. W.; Andres, J. L.; Gonzalez, C.; Head-Gordon, M.; Replogle, E. S.; Pople, J. A. *Gaussian 98*, revision A.5; Gaussian, Inc.: Pittsburgh, PA, 1998.

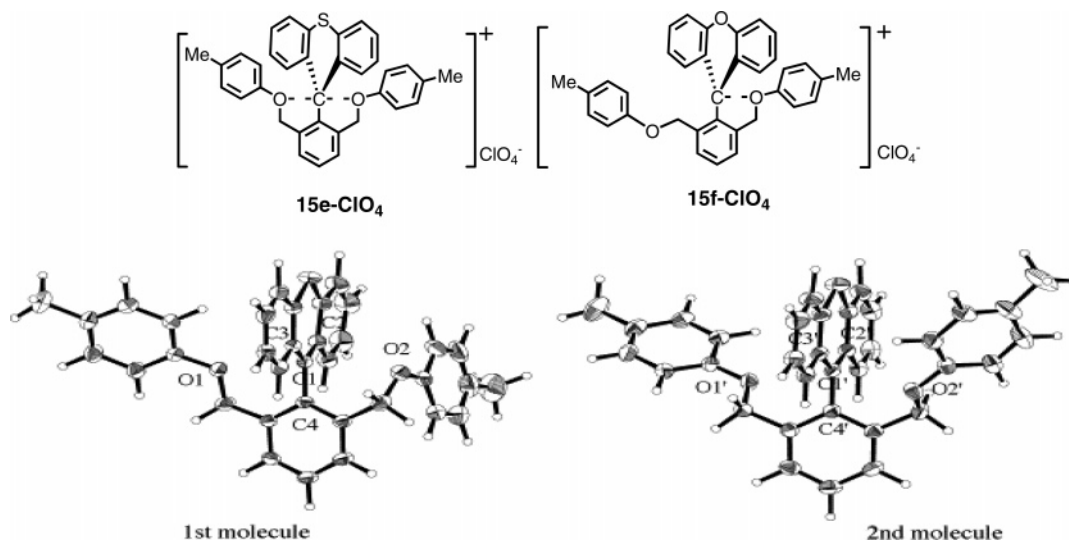


Figure 7. ORTEP drawing of **15e-ClO₄**.

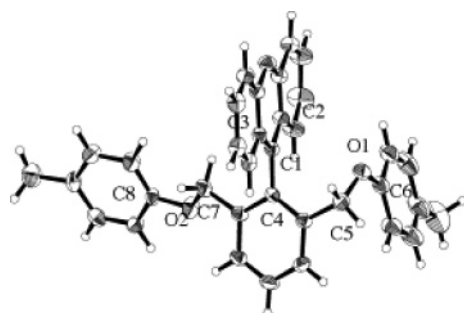


Figure 8. ORTEP drawing of **15f-ClO₄**.

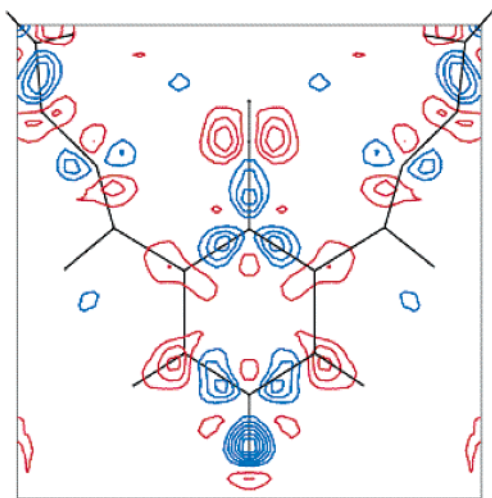


Figure 9. Static model map of **15b-ClO₄** based on the accurate X-ray analysis. Positive and negative regions are shown as blue and red lines, respectively, and zero contours are omitted.

(C⁸–O²–C⁷). One of the two peaks is extended to the central carbon atom. The hole of the 2p orbital appears as electron-deficient regions (marked in red) at both sides of the sp² plane of the central carbon atom and has lobes extended perpendicular to the plane. One of the two lone pairs in the sp³ orbital on each O atom is directed to the empty 2p orbital of the central carbon atom. Such geometry of the orbital clearly indicates that the electrons are donated from the lone pairs in the sp³ orbital

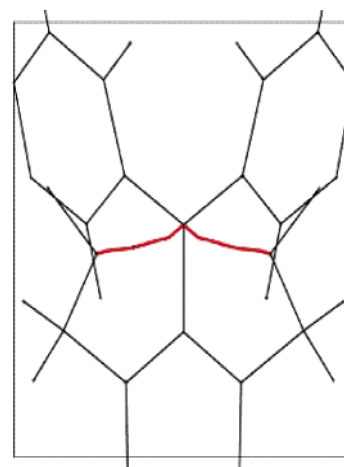


Figure 10. Bond paths of **15b-ClO₄** between the central carbon and the oxygen of the arm based on the accurate X-ray analysis.

on the O atom to the empty 2p orbital of the central carbon atom, thus forming a three-center four-electron bond.

For the quantitative treatment of the characterization of the bonds, topological analyses were performed. The bond paths (shown as red lines) were found between the central carbon and the oxygen of the arm as shown in Figure 10. The shapes of the bond paths of the two bonds are identical. The bond critical points on each bond path are closer to the central carbon atom than the O atoms because of the polarities of the bonds. The small electron density ($\rho(r)$; 0.0170(4) e/a₀³; a₀ = 0.529177 Å) and the small positive Laplacian ($\nabla^2\rho(r)$; 0.0486(1) e/a₀⁵) value at the bond critical point indicate that the bond is weak and polarized. These values are very similar to the values for the C–O bond in our hypervalent five-coordinate carbon compound (**1**) ($\rho(r)$, 0.022 e/a₀³; $\nabla^2\rho(r)$, 0.080 e/a₀⁵).⁸ The difference between the present substituted benzene system and the anthracene system, especially the decrease in the $\rho(r)$ and $\nabla^2\rho(r)$ values, implies an even weaker bond in the present substituted benzene system. Further investigation toward the quantitative estimation of the attractive force is underway.

Electron-Density Distribution Study in 15b-ClO₄ by Density Functional Calculation. The structure of **15b-ClO₄** was optimized with hybrid density functional theory (DFT) at

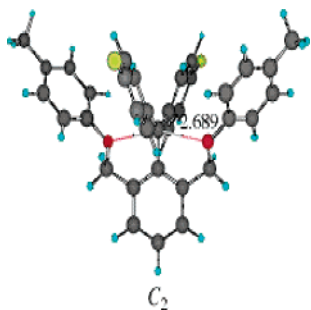


Figure 11. Optimized structure of **15b-ClO₄** at the B3PW91/6-31G(d) level.

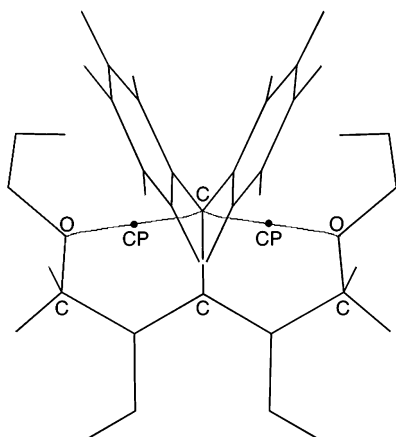


Figure 12. Bond paths of **15b-ClO₄** between the central carbon and the oxygen of the arm calculated at the B3PW91/6-31G(d) level.

the B3PW91/6-31G(d) level,¹² using the Gaussian 98 program.¹³ The basis sets employed were 6-31G(d)¹⁴ for C, O, F, and H. The calculation indicates that the symmetrical C₂ structure of **15b-ClO₄** is the energy minimum (Figure 11). The two C–O distances are almost identical (2.689 Å) to the experimental distances (2.6822(4) Å). It should be noted that the bond paths are also found between the central carbon atom and the two oxygen atoms by the calculation (Figure 12), and the path is well consistent with the one by detailed X-ray analysis previously described. In addition, the small $\rho(r)$ value of 0.017 e/a_0^3 and the small positive $\nabla^2\rho(r)$ value of 0.052 e/a_0^5 calculated at the bond critical points agree well with those of 0.0170(4) e/a_0^3 and 0.0486(1) e/a_0^5 by the accurate X-ray analysis, respectively.

Conclusion

The present series of sterically flexible substituted benzenes showed the sensitivity of the C–O interaction to the electronic effect on the central carbocation, and this was exemplified by the X-ray analysis of these compounds. The X-ray data represent a series of stable pentacoordinate carbon structures, in which the central carbon equally attracts the two apical ligands, to varying extents. The remarkable coincidence of quantitative values obtained by accurate X-ray analysis and DFT calculation is certainly noteworthy here.

Experimental Section

Synthesis of 2,6-Bis(methylthiomethyl)bromobenzene (5a). To a 500 mL round-bottom flask fitted with a reflux condenser was added aqueous sodium methanethiolate (15%, 280 g, 660 mmol), and then

was added an CH₃CN solution (120 mL) of 2,6-bis(bromomethyl)-bromobenzene **4** (20.8 g, 60.7 mmol). The reaction mixture was heated to reflux for 14 h. The crude oil was treated with saturated aqueous NH₄Cl, and the organic layer was distilled to give pure **5a** (62.6 g, 63%) as a pale yellow oil. Compound **5a**: bp 105–106 °C/0.3 Torr; MS m/z 277 (M⁺). ¹H NMR (CDCl₃) δ 2.28 (s, 6H), 3.53 (s, 4H), 7.22 (t, 1H, $J = 8$ Hz), 7.31 (d, 2H, $J = 8$ Hz). ¹³C NMR (CDCl₃) δ 45.3, 63.6, 126.3, 126.6, 129.0, 138.3.

General Procedures for Synthesis of 6. To a THF (10 mL) solution of **5** (1 mmol) was added dropwise *n*-BuLi (1.05 mL, 1.20 M in hexane, 1.26 mmol) at –78 °C under Ar, and the solution was stirred for 1 h. To the reaction mixture was added dropwise a THF (6 mL) solution of a ketone (1 mmol) at –78 °C. The mixture was allowed to warm to room temperature and was stirred for 3–6 h. The mixture was treated with saturated aqueous NH₄Cl. The crude product was purified by silica gel chromatography or recycling HPLC.

General Procedures for Synthesis of 7. To a solution of **6** (0.3 mmol) in diethyl ether (5 mL) were added a few drops of 70% perchloric acid (0.25 mL, 0.4 mmol) under Ar at room temperature. After the mixture was stirred for 2 h, the resulting precipitates were washed with diethyl ether (5 mL \times 3).

Diphenyl[2,6-bis(methylthiomethyl)phenyl]methyl Perchlorate (7a-ClO₄). Yield 80%, colorless crystals; mp 135–137 °C. ¹H NMR (CD₃CN, –40 °C) δ 1.45 (s, 3H), 2.25 (s, 3H), 3.13 (s, 2H), 4.71 (d, $J = 17$ Hz, 1H), 5.01 (d, $J = 17$ Hz, 1H), 7.40–7.70 (m, 13H). ¹³C NMR (CD₃CN, –40 °C) δ 11.9, 22.2, 32.2, 43.4, 85.6, 123.9, 126.7, 126.8, 127.0, 127.5, 127.9, 128.2, 128.3, 129.1, 132.9, 133.3, 134.5, 134.9. Anal. Calcd for C₂₃H₂₃ClO₄S₂: C, 59.66; H, 5.01. Found: C, 59.32; H, 4.88.

General Procedures for Synthesis of 13 and 14. To a THF (10 mL) solution of **11** or **12** (1 mmol) was added dropwise *n*-BuLi (1.05 mL, 1.20 M in *n*-hexane, 1.26 mmol) at –78 °C under Ar, and the solution was stirred for 1 h. To the reaction mixture was added dropwise a THF (5 mL) solution of a ketone (1 mmol) at –78 °C. The mixture was allowed to warm to room temperature and was stirred for 3–6 h. The mixture was treated with saturated aqueous NH₄Cl. The crude product was purified by silica gel chromatography or recycling HPLC.

Diphenyl[2,6-bis(*p*-methylphenoxy)methyl]phenyl]methanol (13a). Yield 58%, colorless crystals (recrystallized from *n*-hexane); mp 115.5–117.0 °C. ¹H NMR (CDCl₃) δ 2.21 (s, 6H), 3.55 (s, 1H), 4.61 (s, 4H), 6.36 (d, 4H, $J = 8$ Hz), 6.89 (d, 4H, $J = 8$ Hz), 7.22 (s, 10H), 7.39 (t, 1H, $J = 8$ Hz), 7.58 (d, 2H, $J = 8$ Hz). Anal. Calcd for C₃₅H₃₂O₃: C, 83.97; H, 6.44. Found: C, 84.12; H, 6.18.

Bis(*p*-fluorophenyl)[2,6-bis(*p*-methylphenoxy)methyl]phenyl]methanol (13b). Yield 49%, colorless crystals (recrystallized from *n*-hexane); mp 112.6–113.8 °C. ¹H NMR (CDCl₃) δ 2.23 (s, 6H), 3.91 (s, 1H), 4.59 (s, 4H), 6.39 (d, 4H, $J = 9$ Hz), 6.93 (d, 4H, $J = 9$ Hz), 6.98 (d, 4H, $J = 9$ Hz), 7.26–7.29 (m, 4H), 7.39 (t, 1H, $J = 8$ Hz), 7.59 (d, 2H, $J = 8$ Hz). FAB(+)MS M⁺ 536.

Bis(*p*-chlorophenyl)[2,6-bis(*p*-methylphenoxy)methyl]phenyl]methanol (13c). Yield 53%, colorless crystals (recrystallized from *n*-hexane); mp 46.7–48.2 °C. ¹H NMR (CDCl₃) δ 2.33 (s, 6H), 4.06 (s, 1H), 4.57 (s, 4H), 6.38 (d, 4H, $J = 8$ Hz), 6.93 (d, 4H, $J = 8$ Hz), 7.22 (s, 8H), 7.39 (t, 1H, $J = 8$ Hz), 7.58 (d, 2H, $J = 8$ Hz). ¹³C NMR (CDCl₃) δ 20.45, 69.62, 82.51, 114.20, 128.06, 128.31, 129.17, 129.60, 129.87, 130.04, 130.27, 133.69, 136.70, 142.61, 144.52, 155.59, 181.21. FAB(+)MS 568, 551, 461, 443, 353. Anal. Calcd for C₃₅H₃₀Cl₂O₃: C, 73.81; H, 5.31. Found: C, 73.86; H, 5.22.

Diphenyl[2,6-bis(*p*-methoxyphenoxy)methyl]phenyl]methanol (14a). Yield 65%. ¹H NMR (CDCl₃) δ 3.64 (s, 1H), 3.71 (s, 6H), 4.59 (s, 4H), 6.40 (d, 4H, $J = 9$ Hz), 6.65 (d, 4H, $J = 9$ Hz), 7.31 (s, 10H), 7.37 (t, 1H, $J = 8$ Hz), 7.61 (d, 2H, $J = 8$ Hz). Anal. Calcd for C₃₅H₃₂O₅: C, 78.93; H, 6.06. Found: C, 78.66; H, 5.95.

Bis(*p*-fluorophenyl)[2,6-bis(*p*-methoxyphenoxy)methyl]phenyl]methanol (14b). Yield 67%, pale yellow solid; mp 38.2–39.0 °C. ¹H NMR (CDCl₃) δ 3.72 (s, 6H), 4.03 (s, 1H), 4.57 (s, 4H), 6.43 (d, 4H,

(14) Francl, M. M.; Pietro, W. J.; Hehre, W. J.; Binkley, J. S.; Gordon, M. S.; DeFrees, D. J.; Pople, J. A. *J. Chem. Phys.* **1982**, *77*, 3654–3665.

$J = 9$ Hz), 6.68 (d, 4H, $J = 9$ Hz), 6.94–6.98 (m, 4H), 7.26–7.28 (m, 4H), 7.40 (t, 1H, $J = 8$ Hz), 7.59 (d, 2H, $J = 8$ Hz). Anal. Calcd for $C_{35}H_{30}F_2O_5$: C, 73.93; H, 5.32. Found: C, 73.76; H, 5.25.

Bis(*p*-chlorophenyl)[2,6-bis(*p*-methoxyphenoxy)methyl]phenyl]methanol (14c). Yield 50%, pale yellow solid; mp 45–49 °C. 1H NMR ($CDCl_3$) δ 3.73 (s, 6H), 4.17 (s, 1H), 4.56 (s, 4H), 6.42 (d, 4H, $J = 9$ Hz), 6.69 (d, 4H, $J = 9$ Hz), 7.23 (s, 8H), 7.41 (t, 1H, $J = 8$ Hz), 7.59 (d, 2H, $J = 8$ Hz). Anal. Calcd for $C_{35}H_{30}Cl_2O_5$: C, 69.89; H, 5.03. Found: C, 69.50; H, 4.66.

Bis(*p*-methoxyphenyl)[2,6-bis(*p*-methoxyphenoxy)methyl]phenyl]methanol (14d). Yield 40%. 1H NMR ($CDCl_3$) δ 3.56 (s, 1H), 3.69 (s, 6H), 3.75 (s, 6H), 4.61 (s, 4H), 6.43 (d, 4H, $J = 9$ Hz), 6.65 (d, 4H, $J = 9$ Hz), 6.79 (d, 4H, $J = 9$ Hz), 7.19 (d, 4H, $J = 9$ Hz), 7.34 (t, 1H, $J = 8$ Hz), 7.59 (d, 2H, $J = 8$ Hz). Anal. Calcd for $C_{37}H_{36}O_7$ + benzene: C, 76.99; H, 6.31. Found: C, 77.01; H, 6.20.

General Procedures for Synthesis of 15 and 16. To a solution of **13** or **14** (0.07 mmol) in CH_2Cl_2 (2.5 mL) were added a few drops of 70% perchloric acid under Ar at -15 °C. After the mixture was stirred for 1 h, the additional CH_2Cl_2 (10 mL) was added slowly, and the reaction mixture was passed through a column of anhydrous Na_2SO_4 to remove excess perchloric acid and water under Ar while keeping the column at the same temperature. The solvent was deliberately removed by Ar flow at -20 °C to precipitate the desired perchlorate salts of carbenium cation as purple plates.

Diphenyl[2,6-bis(*p*-methylphenoxy)methyl]phenyl]methyl Perchlorate (15a-ClO₄). 1H NMR ($CDCl_3$) δ 2.21 (s, 6H), 4.45 (brs, 4H), 5.99 (d, 4H, $J = 8$ Hz), 6.82 (d, 4H, $J = 8$ Hz), 7.5–7.7 (m, 11H, $J = 9$ Hz), 8.15 (d, 2H, $J = 8$ Hz).

Bis(*p*-fluorophenyl)[2,6-bis(*p*-methylphenoxy)methyl]phenyl]methyl Perchlorate (15b-ClO₄). mp 114.9–115.6 °C (dec) (recrystallized from CH_2Cl_2/Et_2O). 1H NMR (CD_2Cl_2) δ 2.22 (s, 6H), 4.51 (br, 4H), 6.04 (d, 4H, $J = 8$ Hz), 6.90 (d, 4H, $J = 8$ Hz), 7.30 (br, 4H), 7.59 (br, 4H), 7.71 (d, 2H, $J = 8$ Hz), 7.87 (t, 1H, $J = 8$ Hz). Anal. Calcd for $C_{35}H_{29}ClF_2O_6 + 0.5CH_2Cl_2$: C, 64.36; H, 4.72. Found: C, 64.64; H, 4.28.

Bis(*p*-chlorophenyl)[2,6-bis(*p*-methylphenoxy)methyl]phenyl]methyl Perchlorate (15c-ClO₄). mp 97.6–100.4 °C (dec) (recrystallized from CH_2Cl_2/Et_2O). 1H NMR (CD_2Cl_2) δ 2.22 (s, 6H), 4.51 (br, 4H), 6.04 (d, 4H, $J = 8$ Hz), 6.90 (d, 4H, $J = 8$ Hz), 7.30 (br, 4H), 7.59 (br, 4H), 7.71 (d, 2H, $J = 8$ Hz), 7.87 (t, 1H, $J = 8$ Hz). ^{13}C NMR (CD_2Cl_2 , -15 °C) δ 20.32, 66.23, 112.12, 129.25, 129.93, 130.46 (br), 131.28 (br), 132.38, 134.39, 134.60, 135.50, 139.07, 140.04 (br), 140.61 (br), 152.56, 153.68, 211.88. UV–vis (CH_2Cl_2 , -15 °C) $\lambda(\epsilon_{max})$ 623.0 (266), 460.5 (2364), 351.5 (692), 337.5 (679), 267.5 (591). Anal. Calcd for $C_{35}H_{29}Cl_3O_6 + 0.5CH_2Cl_2$: C, 62.02; H, 4.55. Found: C, 61.94; H, 4.22.

9-[2,6-Bis(*p*-methylphenoxy)methyl]phenyl]thioxanthylum Perchlorate (15e-ClO₄). 1H NMR ($CDCl_3$) δ 2.08 (s, 6H), 4.62 (s, 4H), 5.69 (d, 4H, $J = 9$ Hz), 6.62 (d, 4H, $J = 9$ Hz), 7.73–7.85 (m, 5H), 7.93 (d, 2H, $J = 9$ Hz), 8.19–8.23 (m, 2H), 8.60 (d, 2H, $J = 9$ Hz).

9-[2,6-Bis(*p*-methylphenoxy)methyl]phenyl]xanthylum Perchlorate (15f-ClO₄). 1H NMR ($CDCl_3$) δ 2.09 (s, 6H), 4.80 (s, 4H), 5.71 (d, 4H, $J = 9$ Hz), 6.64 (d, 4H, $J = 9$ Hz), 7.69–7.84 (m, 7H), 8.18 (d, 2H, $J = 9$ Hz), 8.38–8.42 (m, 2H).

Diphenyl[2,6-bis(*p*-methoxyphenoxy)methyl]phenyl]methyl Perchlorate (16a-ClO₄). mp 108.0–109.0 °C (recrystallized from CH_2Cl_2/Et_2O). 1H NMR (CD_2Cl_2) δ 3.68 (s, 6H), 4.44 (s, 4H), 6.04 (d, 4H, $J = 9$ Hz), 6.59 (d, 4H, $J = 9$ Hz), 7.35–7.75 (br, 10H), 7.60–7.90 (br, 1H), 8.05–8.22 (br, 2H). UV–vis (CH_2Cl_2 , -15 °C) $\lambda(\epsilon_{max})$ 677.0 (331), 426.5 (1814), 330 (729), 291 (516). Anal. Calcd for $C_{35}H_{31}ClO_8$: C, 68.23; H, 5.24. Found: C, 67.96; H, 4.92.

Bis(*p*-fluorophenyl)[2,6-bis(*p*-methoxyphenoxy)methyl]phenyl]methyl Hexafluorophosphate (16b-PF₆). mp 128.0–129.0 °C. (recrystallized from CH_2Cl_2/Et_2O). 1H NMR (CD_2Cl_2) δ 3.66 (s, 6H), 4.42

(s, 4H), 6.03 (d, 4H, $J = 9$ Hz), 6.59 (d, 4H, $J = 9$ Hz), 7.20–7.80 (br, 6H), 7.60–7.90 (br, 2H), 7.67 (d, 2H, $J = 8$ Hz), 7.83 (t, 1H, $J = 8$ Hz). UV–vis (CH_2Cl_2 , -15 °C) $\lambda(\epsilon_{max})$ 600.5 (287), 467.0 (3184), 335 (687), 290 (537). Anal. Calcd for $C_{35}H_{29}F_8O_4P$: C, 60.35; H, 4.20. Found: C, 60.03; H, 3.84.

Bis(*p*-chlorophenyl)[2,6-bis(*p*-methoxyphenoxy)methyl]phenyl]methyl hexafluorophosphate (16c-PF₆). mp 116.5–117.8 °C. (recrystallized from CH_2Cl_2/Et_2O). 1H NMR (CD_2Cl_2) δ 3.70 (s, 6H), 4.49 (s, 4H), 6.10 (d, 4H, $J = 9$ Hz), 6.63 (d, 4H, $J = 9$ Hz), 7.42 (br, 4H), 7.57 (br, 4H), 7.70 (br, 2H), 7.85 (br, 1H). UV–vis (CH_2Cl_2 , -15 °C) $\lambda(\epsilon_{max})$ 715.0 (359), 458.0 (3312), 350.5 (1093), 341.5 (1033), 290.5 (703). Anal. Calcd for $C_{35}H_{29}Cl_2F_6O_4P + 0.5CH_2Cl_2$: C, 55.23; H, 3.92. Found: C, 55.52; H, 3.44.

Bis(*p*-methoxyphenyl)[2,6-bis(*p*-methoxyphenoxy)methyl]phenyl]methyl Hexafluorophosphate (16d-PF₆). mp 144.0–146.0 °C. (recrystallized from CH_2Cl_2/Et_2O). 1H NMR (CD_2Cl_2) δ 3.68 (s, 6H), 4.08 (s, 6H), 4.47 (s, 4H), 6.21 (d, 4H, $J = 9$ Hz), 6.63 (d, 4H, $J = 9$ Hz), 7.05 (d, 4H, $J = 9$ Hz), 7.48 (d, 4H, $J = 9$ Hz), 7.66 (d, 2H, $J = 9$ Hz), 7.76 (d, 4H, $J = 9$ Hz). UV–vis (CH_2Cl_2 , -15 °C) $\lambda(\epsilon_{max})$ 715.0 (359), 458.0 (3312), 350.5 (1093), 341.5 (1033), 290.5 (703). Anal. Calcd for $C_{37}H_{35}F_6O_6P$: C, 61.67; H, 4.90. Found: C, 61.80; H, 4.23.

X-ray Crystallographic Analysis of 7c-ClO₄, 15b-ClO₄, 15c-ClO₄, 15e-ClO₄, 15f-ClO₄, 16a-ClO₄, 16b-PF₆, and 16d-PF₆. X-ray data, except experimental electron distribution analysis, were collected on a Mac Science DIP2030 imaging plate equipped with graphite-monochromated Mo K α radiation ($\lambda = 0.71073$ Å). The unit cell parameters were determined by autoindexing several images in each data set separately with the program DENZO. For each data set, rotation images were collected in 3° increments with a total rotation of 180° about ϕ . Data were processed by SCALEPACK. The structures were solved using the teXsan system and were refined by full-matrix least-squares and refined by full-matrix least-squares. The programs DENZO and SCALEPACK are available from Mac Science Co., Z. Otwinowski, University of Texas, Southwestern Medical Center. The program teXsan is available from Rigaku Co. All crystallographic data (excluding structure factors) for the compounds reported in this paper have been deposited with the Cambridge Crystallographic Data Centre (all data have a supplementary publication number). A copy of the data can be obtained free of charge on application to CCDC, 12 Union Road, Cambridge CB2 1EZ, UK (fax, (+44)1223-336-033; e-mail, deposit@ccdc.cam.ac.uk).

7c-ClO₄ (deposited as CCDC-251373): $C_{35}H_{31}O_4S_2Cl$, 615.20, monoclinic, $P2_1/n$, pale yellow, $a = 14.4590(9)$ Å, $b = 11.522(1)$ Å, $c = 19.651(2)$ Å, $\beta = 109.542(5)^\circ$, $V = 3085.2(4)$ Å³, 298 K, $Z = 4$, $R = 0.1059$, GOF = 1.882.

15b-ClO₄ (deposited as CCDC-251374): $C_{35}H_{29}O_6F_2Cl$, 619.06, orthorhombic, $Pbcn$, red purple, $a = 11.8900(6)$ Å, $b = 14.0860(4)$ Å, $c = 17.8700(9)$ Å, $V = 2992.9(2)$ Å³, 298 K, $Z = 4$, $R = 0.0649$, GOF = 1.364.

15c-ClO₄ (deposited as CCDC-251375): $C_{35}H_{29}O_6Cl_3$, 651.97, orthorhombic, $Pna2_1$, brown purple, $a = 18.4610(5)$ Å, $b = 13.9050(3)$ Å, $c = 12.3370(7)$ Å, $V = 3166.9(1)$ Å³, 298 K, $Z = 4$, $R = 0.0580$, GOF = 1.327.

15e-ClO₄ (deposited as CCDC-251376): $C_{35}H_{29}O_6S_2Cl$, 613.12, triclinic, $P\bar{1}$, purple, $a = 11.5140(2)$ Å, $b = 15.3280(5)$ Å, $c = 18.5310(6)$ Å, $\alpha = 78.168(1)^\circ$, $\beta = 78.935(2)^\circ$, $\gamma = 79.867(2)^\circ$, $V = 3109.6(2)$ Å³, 200 K, $Z = 4$, $R = 0.0908$, GOF = 1.658.

15f-ClO₄ (deposited as CCDC-251377): $C_{35}H_{29}O_7Cl$, 597.06, triclinic, $P\bar{1}$, purple, $a = 11.335(2)$ Å, $b = 11.064(2)$ Å, $c = 13.066(1)$ Å, $\alpha = 101.128(9)^\circ$, $\beta = 102.83(1)^\circ$, $\gamma = 102.734(5)^\circ$, $V = 1507.14(4)$ Å³, 200 K, $Z = 4$, $R = 0.1063$, GOF = 1.583.

16a-ClO₄ (deposited as CCDC-251378): $C_{35}H_{31}O_8Cl_3$, 615.08, monoclinic, $C2/c$, purple, $a = 15.062(8)$ Å, $b = 20.078(1)$ Å, $c = 11.4130(4)$ Å, $\beta = 114.277(3)^\circ$, $V = 3146.2(3)$ Å³, 298 K, $Z = 4$, $R = 0.0788$, GOF = 1.664.

16b-PF₆ (deposited as CCDC-251379): C₃₅H₃₁O₈Cl₃, 696.57, orthorhombic, *Pbcn*, purple, $a = 12.7300(5)$ Å, $b = 14.06090(6)$ Å, $c = 17.6890(7)$ Å, $V = 3289.7(2)$ Å³, 298 K, $Z = 4$, $R = 0.1548$, GOF = 2.521.

16d-PF₆ (deposited as CCDC-251380): C₃₇H₃₅O₆F₆P, 720.64, monoclinic, *P2₁/n*, red purple, $a = 13.5070(4)$ Å, $b = 17.866(1)$ Å, $c = 14.6090(9)$ Å, $\beta = 91.321(3)^\circ$, $V = 3524.4(3)$ Å³, 298 K, $Z = 4$, $R = 0.1616$, GOF = 2.584.

Accurate X-ray Analysis of 15b-CIO₄. A single crystal of **15b-CIO₄** having well-developed crystal faces, $0.24 \times 0.21 \times 0.10$ mm, was selected for measurement. Diffraction data were collected on an automated imaging plate Weissenberg camera, MacScience DIP-LABO, on BL04B2 beam line at SPring-8¹⁵ using 37.8 keV (0.3282 Å) radiation with an oscillation method at 100 K. Sixty frames were measured with an oscillation angle of 4° and an interval of 3° to ensure a total oscillation angle of 180°. Bragg spots on the imaging plates were integrated up to $\sin \theta/\lambda = 1.0$ Å⁻¹ with the program DENZO and scaled and averaged with the program SCALEPACK. Partial reflections were omitted. Lorentz and polarization corrections were applied during the scaling process. Absorption correction was not applied due to the low absorptivity of the specimen. Measured and independent reflections, R_{int} , and completeness were 108928, 11503, 0.03, and 0.94, respectively.

The structure was solved by a direct method and refined using independent 3348 reflections with $\sin \theta/\lambda \leq 0.65$ Å⁻¹ with the programs SIR97¹⁶ and SHELXL97,¹⁷ respectively. Following the refinements, high-order refinements were carried out using all 8823 independent reflections with $\sin \theta/\lambda \geq 0.60$ Å⁻¹ with the program SHELXL97. The positions of the hydrogen atoms were constrained to have C–H distances of 1.083 and 1.066 Å for aromatic and methyl groups, respectively.¹⁸ Refinements of the multipole expansion method using the Hansen–Coppens multipole formalism¹⁹ and topological analyses based on the resulting parameters were performed with the XD

package.²⁰ The refinement was carried out against 11 095 independent reflections of $\sin \theta/\lambda \leq 1.0$ Å⁻¹ with $I > 0$ based on F^2 . At the first stage of the refinements, atomic coordinates and U_{ij} of non-hydrogen atoms were fixed on those of the high order refinement, and the U_{iso} values of the hydrogen atoms were fixed on those of the conventional refinements based on reflections with $\sin \theta/\lambda \leq 0.65$ Å⁻¹. The population parameters, P_v , $P_{\text{lm}\pm}$, of non-hydrogen atoms and scale were refined. Levels of multipoles were raised stepwise up to hexadecapole for the non-hydrogen atoms. At the second stage, anisotropic and isotropic temperature factors were refined for non-hydrogen and hydrogen atoms, respectively, followed by the spherical Hartree–Fock radial screening parameter, κ . At the third stage, the P_v , $P_{\text{lm}\pm}$, and scale were refined. The levels of multipoles were raised to the hexadecapole for non-hydrogen atoms and to the dipole along the bonds for hydrogen atoms in the same manner at the final stage. After those refinements, the second and third strategies were repeated twice, and finally the P_v , $P_{\text{lm}\pm}$, κ , coordinates, and temperature factors and scale were refined. The number of parameters in the final cycle of the refinements was 852. A molecule electroneutrality constraint was applied through all of the refinements. Crystal data: orthorhombic, space group *Pbcn*, $a = 11.853(1)$ Å, $b = 14.003(1)$ Å, $c = 17.725(1)$ Å, $V = 2942.0(4)$ Å³, $Z = 4$, $D_x = 1.398$ g cm⁻³, $R(F) = 0.0281$ (for 11 095 reflections with $I > 0$).

Acknowledgment. This work was supported by a Grant-in-Aid for Scientific Research (Nos. 09239103, 11166248, 11304044) from the Ministry of Education, Science, Sports, and Culture of the Japanese Government. Measurement of diffraction data for electron density analysis of **15b-CIO₄** was carried out at SPring-8 under project number 2001A-0229-ND-np.

Supporting Information Available: Preparation of compounds and tables of crystal data, structure solution and refinement, atomic coordinates, anisotropic thermal parameters, and bond distances and angles. This material is available free of charge via the Internet at <http://pubs.acs.org>.

JA043802T

- (15) Ozeki, T.; Kusaka, K.; Honma, N.; Nakamura, Y.; Nakamura, S.; Oike, S.; Yasuda, N.; Imura, H.; Uekusa, H.; Isshiki, M.; Katayama, C.; Ohashi, Y. *Chem. Lett.* **2001**, 804.
- (16) Altomare, A.; Burla, M. C.; Camalli, M.; Cascarano, G. L.; Giacovazzo, C.; Guagliardi, A.; Moliterni, A. G. G.; Polidori, G.; Spagna, R. *J. Appl. Cryst.* **1999**, 32, 115.
- (17) Sheldrick, G. M. *SHELX-97, Program for the Analysis of Crystal Structures*; University of Göttingen: Göttingen, Germany, 1997.
- (18) Wilson, A. J. C. *International Tables for Crystallography* Kluwer Academic Publishers: Dordrecht, 1992; Vol. C.
- (19) (a) Coppens, P. *X-ray Charge Densities and Chemical Bonding*; Oxford University Press: New York, 1997. (b) Hansen, N. K.; Coppens, P. *Acta Crystallogr., Sect. A* **1978**, 34, 909.

- (20) Koritsanszky, T.; Howard, S.; Su, Z.; Mallinson, P. R.; Richter, T.; Hansen, N. K. *XD—a Computer Program Package for Multipole Refinement and Analysis of Electron Densities from Diffraction Data*; 2003.